Am J Physiol Heart Circ Physiol 288: H2363–H2374, 2005.
First published December 22, 2004; doi:10.1152/ajpheart.00348.2004.

Unique modulation of L-type Ca^{2+} channels by short auxiliary β_{1d} subunit present in cardiac muscle

Risa M. Cohen,[2,*] Jason D. Foell,[1,*] Ravi C. Balijepalli,[1] Vaibhavi Shah,[3] Johannes W. Hell,[3] and Timothy J. Kamp[1,2]

Departments of [1]Medicine and [2]Physiology, University of Wisconsin, Madison, Wisconsin; and [3]Department of Pharmacology, University of Iowa, Iowa City, Iowa

Submitted 12 April 2004; accepted in final form 21 December 2004

Cohen, Risa M., Jason D. Foell, Ravi C. Balijepalli, Vaibhavi Shah, Johannes W. Hell, and Timothy J. Kamp. Unique modulation of L-type Ca^{2+} channels by short auxiliary β_{1d} subunit present in cardiac muscle. *Am J Physiol Heart Circ Physiol* 288: H2363–H2374, 2005. First published December 22, 2004; doi:10.1152/ajpheart.00348.2004.—Recent studies have identified a growing diversity of splice variants of auxiliary Ca^{2+} channel $Ca_v\beta$ subunits. The $Ca_v\beta_{1d}$ isoform encodes a putative protein composed of the amino-terminal half of the full-length $Ca_v\beta_1$ isoform and thus lacks the known high-affinity binding site that recognizes the Ca^{2+} channel α_1-subunit, the α-binding pocket. The present study investigated whether the $Ca_v\beta_{1d}$ subunit is expressed at the protein level in heart, and whether it exhibits any of the functional properties typical of full-length $Ca_v\beta$ subunits. On Western blots, an antibody directed against the unique carboxyl terminus of $Ca_v\beta_{1d}$ identified a protein of the predicted molecular mass of 23 kDa from canine and human hearts. Immunocytochemistry and surface-membrane biotinylation experiments in transfected HEK-293 cells revealed that the full-length $Ca_v\beta_{1b}$ subunit promoted membrane trafficking of the pore-forming α_{1C} ($Ca_v1.2$)-subunit to the surface membrane, whereas the $Ca_v\beta_{1d}$ subunit did not. Whole cell patch-clamp analysis of transfected HEK-293 cells demonstrated no effect of coexpression of the $Ca_v\beta_{1d}$ with the α_{1C}-subunit compared with the 15-fold larger currents and leftward shift in voltage-dependent activation induced by full-length $Ca_v\beta_{1b}$ coexpression. In contrast, cell-attached patch single-channel studies demonstrated that coexpression of either $Ca_v\beta_{1b}$ or $Ca_v\beta_{1d}$ significantly increased mean open probability four- to fivefold relative to the α_{1C}-channels alone, but only $Ca_v\beta_{1b}$ coexpression increased the number of channels observed per patch. In conclusion, the $Ca_v\beta_{1d}$ isoform is expressed in heart and can modulate the gating of L-type Ca^{2+} channels, but it does not promote membrane trafficking of the channel complex.

electrophysiology; ion; heart; splice variant

CALCIUM CHANNELS ARE FOUND IN many excitable tissues and are intricately involved in important cellular processes including genesis of action potentials, excitation-contraction coupling, and gene expression. Voltage-dependent Ca^{2+} channels are multisubunit proteins that consist of a pore-forming α_1-subunit that is associated with auxiliary subunits including the cytoplasmic β-subunit, a membrane-associated $\alpha_2\delta$-subunit, and a γ-subunit (10). The ultimate functional properties of Ca^{2+} channels are determined not only by the pore-forming α_1-subunits but also by the combination of auxiliary subunits that finely tune the channel properties.

The auxiliary Ca^{2+} channel $Ca_v\beta$ subunit is encoded by four different genes with a rich array of alternatively spliced isoforms that are expressed in a tissue- and species-specific pattern (6). For example, in canine and human ventricles, we have previously found (20) evidence for a total of 18 different $Ca_v\beta$ isoforms. The genes typically encode proteins of 400–600 amino acids in length and are composed of five general domains (Fig. 1). Domains 2 and 4 are widely conserved across all four $Ca_v\beta$ genes and contain Src homology-3 (SH3) and guanylate kinase (GK) motifs, respectively. Recent crystallographic studies (11, 35, 45) have demonstrated that $Ca_v\beta$ subunits are members of the membrane-associated guanylate kinase (MAGUK) family of scaffolding proteins, which are characterized by closely interacting SH3 and GK domains. High-affinity binding of $Ca_v\beta$ subunits to the α_1-subunit occurs in a hydrophobic groove in the $Ca_v\beta$ subunit GK domain that is referred to as the α-binding pocket (ABP). All full-length $Ca_v\beta$ subunits include a similar core formed by the interacting SH3 and GK domains including the ABP, and variability among the different $Ca_v\beta$ isoforms occurs primarily in domains 1, 3, and 5. In addition, recent studies have also identified short or truncated $Ca_v\beta$ isoforms that result from alternative splicing and a frame shift that causes an early stop codon (20, 25, 26). These short or "d" isoforms are truncated before domain 4, and the resulting proteins are approximately one-half the size as the full-length isoforms and thus lack the GK domain with its high-affinity binding site for the α_1-subunit.

The functional roles of the full-length $Ca_v\beta$ subunits have been extensively explored using heterologous expression studies. $Ca_v\beta$ subunits play critical roles in membrane trafficking of the channel complex and in regulation of voltage-dependent gating (4, 13, 17, 22, 29, 30). The $Ca_v\beta$ subunit binds to the endoplasmic reticulum (ER) retention signal in the I-II loop of the α_1-subunit, which allows channels to traffic to the surface membrane (4). Furthermore, $Ca_v\beta$ subunits not only allow for membrane trafficking of the channel complex; they also can play a role in determining the subcellular localization of channels on the surface membrane (7, 15, 20). $Ca_v\beta$ subunits have been demonstrated to differentially regulate activation, inactivation, recovery from inactivation, and voltage-dependent facilitation of heterologously expressed channels (18, 28–30, 40). Modulation of voltage-dependent gating can be finely

* R. M. Cohen and J. D. Foell contributed equally to this work.

Address for reprint requests and other correspondence: T. J. Kamp, H6/343 Clinical Science Center, Box 3248, 600 Highland Ave., Madison, WI 53792 (E-mail: tjk@medicine.wisc.edu).

The costs of publication of this article were defrayed in part by the payment of page charges. The article must therefore be hereby marked "*advertisement*" in accordance with 18 U.S.C. Section 1734 solely to indicate this fact.

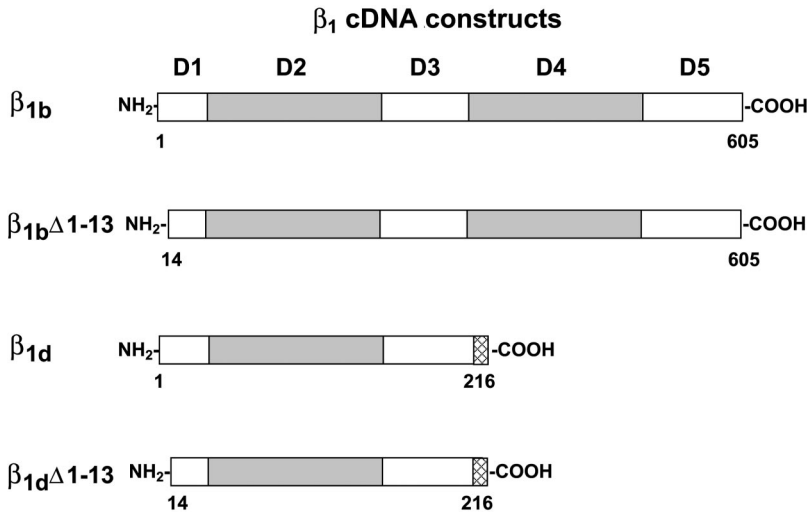

Fig. 1. Structure of human $Ca_v\beta_1$-splice variants and constructs studied. Conserved domains among the four $Ca_v\beta$ subunit genes; gray regions) and variable domains (open bars) are shown. Unique seven amino acids found only in $Ca_v\beta_{1d}$ and not other $Ca_v\beta_1$-splice variants in domain (D) 3 owing to alternative splicing and a frame shift are indicated (cross-hatched areas). $Ca_v\beta_{1d}\Delta1$–13 and $Ca_v\beta_{1b}\Delta1$–13 lack the first 13 amino acids of domain 1.

regulated by different splice variants from the same $Ca_v\beta$ subunit gene. For example, splice variants of $Ca_v\beta_2$ and $Ca_v\beta_4$ genes, which differ only in the proximal NH_2 terminus (domain 1), have distinct effects on channel properties including steady-state activation and voltage-dependent inactivation gating (20, 24, 43).

The shorter splice forms or "d" isoforms of the $Ca_v\beta$ genes have only recently been identified, and their functional properties have not yet been completely characterized. The short isoforms lack the ABP, so their effects on expressed α_1-channels may be quite different or absent compared with full-length $Ca_v\beta$ isoforms. All four $Ca_v\beta$ genes can encode short $Ca_v\beta$ subunits using similar alternative splicing (20, 25, 26), but only the $Ca_v\beta_3$ and $Ca_v\beta_4$ short isoforms have been functionally characterized. In the case of the $Ca_v\beta_4$ gene, a short isoform was shown to be involved in gene regulation and only caused minor changes in voltage-dependent gating (25). The short form of the $Ca_v\beta_3$ isoform did not clearly alter whole cell currents, but at the single-channel level effects on gating were observed (26). No studies have yet proven that the short isoforms are expressed at the protein level in native tissues, including heart. In addition, no investigations have directly addressed whether the short $Ca_v\beta$ subunits promote membrane trafficking of the channel complex compared with full-length $Ca_v\beta$ subunits. Last, no functional characterization of a heterologously expressed short-splice variant from the $Ca_v\beta_1$ gene has been reported.

The purpose of the present work was to determine whether the short $Ca_v\beta_1$ splice variant $Ca_v\beta_{1d}$ is expressed at the protein level in heart and to determine its functional effects on membrane trafficking and voltage-dependent gating of α_{1C}-encoded L-type Ca^{2+} channels. A preliminary account of these studies has been reported (14).

MATERIALS AND METHODS

Heterologous expression of Ca^{2+} channel subunits in HEK-293 cells. HEK-293 cells were cultured in DMEM supplemented with 10% fetal calf serum (Harlan; Indianapolis, IN), 100 U/ml penicillin, 100 μg/ml streptomycin, and 2 mM L-glutamine. The HEK-293 cells were grown on 15-mm glass coverslips coated with type I collagen from rat tails (Sigma; St. Louis, MO) and were transiently transfected with the subunit(s) of interest using the calcium phosphate method (Invitrogen; Carlsbad, CA). The rabbit full-length α_{1C} ($Ca_v1.2$)-subunit (33), except for alternative splicing in domain IV S3 (41), subcloned into pGW1H (British Biotechnology; Oxford, UK), was expressed alone or in a 1:1 molar ratio with human β_{1b}- (GenBank accession no. M92303) or human β_{1d}- (GenBank accession no. AY393857) subunit subcloned into pcDNA3.1. The channel subunits were cotransfected with pSV40Tag to increase expression levels and green fluorescent protein (GFP)pRK5 to identify transfected cells (36). Cells were then used for whole cell electrophysiology or imaging experiments the day after transfection.

β_{1d}-Antibody and Western blot analyses. A polyclonal rabbit anti-$Ca_v\beta_{1d}$ antibody was produced using an epitope specific to the unique COOH terminus of the $Ca_v\beta_{1d}$ subunit (KPASDRACAPL; the NH_2-terminal lysine is not part of the original $Ca_v\beta_{1d}$ sequence but was added to aid in coupling to the carrier). The $Ca_v\beta_{1d}$ COOH-terminal peptide was synthesized, purified, coupled to BSA with glutaraldehyde, and used to immunize rabbits as previously described (50). The resulting antibody was affinity purified on the peptide used for immunization coupled to CNBr-activated Sepharose 4B.

Sarcolemmal-, T-tubular-, and dyadic-enriched membrane fractions (FI, FII, and FIII, respectively) were prepared from canine left ventricular tissue using differential and discontinuous sucrose density-gradient centrifugation (1). Proteins (60 μg) from the isolated canine ventricular membrane fractions and transfected HEK-293 cells were solubulized in sample buffer (that contained 62.5 mM Tris·HCl, pH 6.8, 10% glycerol, 2% SDS, 5% 2-mercaptoethanol, and 0.1% bromophenol blue) by warming to 60°C for 30 min (23) and were separated by SDS-PAGE using 12% bis-acrylamide gels as described by Laemmli (31). After separation, proteins were transferred to a polyvinylidene difluoride membrane (Bio-Rad Laboratories; Hercules, CA) by blotting for 1 h at 105 V. Nonspecific binding sites were blocked by immersion of membranes for 2 h at room temperature in Tris-buffered saline detergent (0.1% Tween-20) that contained 5% (wt/vol) dried skim milk. Membranes were then probed with rabbit polyclonal anti-$Ca_v\beta_{1d}$ primary antibody (1:500 dilution). Goat anti-rabbit immunoglobulin linked to horseradish peroxidase (1:50,000 dilution) detected bound primary antibody. Immunoreactivity was visualized using the ECL peroxidase-based chemiluminescent detection system (Amersham Life Sciences; Cleveland, OH).

Immunofluorescence confocal imaging. Immunolabeling was performed on transiently transfected HEK-293 cells using a rabbit polyclonal antibody directed against α_{1C}-protein (recognizing a region in

the central cytosolic loop between α_{1C}-domains II and III; Ref. 16). Transfected HEK-293 cells grown overnight were initially fixed with 2% paraformaldehyde in PBS for 10 min. Fixed cells were permeabilized with 0.1% Triton X-100 in PBS for 10 min and then quenched for aldehyde groups in 0.75% glycine in PBS for 10 min. After cells were washed with PBS for 2–5 min, they were incubated with 1 ml of blocking solution (that contained 2% BSA, 5% goat serum, and 0.05% NaN_3 in TBS) for 1 h to block nonspecific binding. Subsequently, the cells were incubated with the polyclonal anti-α_{1C}-antibody (a 1:500 dilution) for 2 h in blocking solution at room temperature. Excess primary antibody was washed off with blocking solution (for 3–10 min). Cells were then incubated with Alexa Fluor 568 goat anti-rabbit IgG antibody (a 1:500 dilution, 2 mg/ml for 2 h; Molecular Probes; Eugene, OR), subsequently washed with blocking solution (for 3–10 min), and mounted onto a slide in a 50:50 glycerol-PBS solution. To identify nonspecific binding, control experiments with secondary antibody alone and experiments in mock transfected cells were performed.

Imaging was performed with an MRC 1024 laser scanning confocal microscope equipped with a mixed-gas (Ar-Kr) laser operated by 24-bit LaserSharp software (Bio-Rad). The Bio-Rad system was mounted on a Nikon Diaphot 200 inverted microscope. Acquisition in the red channel utilized excitation at a 568-nm wavelength with emission detected at 605 ± 16 nm. Cells were randomly selected and used for image analysis. Images were scanned using a ×60 objective.

Biotinylation of cell surface protein and immunoblotting. HEK-293 cells were grown in 100-mm culture dishes and individually transfected with the subunit(s) of interest, and the rabbit full-length α_{1C}-subunit was expressed alone or in a 1:1 molar ratio with human β_{1b}- or β_{1d}-subunits. After 48 h, cells were washed three times with PBS at room temperature (22–25°C), and cell surface proteins were biotinylated using the EZ-Link Sulfo-NHS-Biotinylation Kit [0.5 mg/ml sulfo-NHS-(LC)-biotin; Pierce; Rockford, IL] in PBS. After incubation at 4°C for 1 h, cells were washed five times with ice-cold PBS to remove any remaining biotinylation reagent. Cells were then harvested in lysis buffer (that contained 130 mM NaCl, 50 mM Tris·HCl, 2 mM EGTA, 1% Nonidet P-40, and 1% Triton X-100) and protease inhibitors (2 mM phenylmethylsulfonyl fluoride, 50 μg/ml aprotinin, 50 μg/ml benzamidine, 50 μg/ml leupeptin, and 5 μM pepstatin A; Sigma). Lysate proteins were quantified with a bicinchoninic acid assay (Pierce). Proteins (150 μg/reaction) were mixed with anti-α_{1C}-antibody (10 μg) and incubated overnight at 4°C, and then 50 μl of a 1:1 slurry of protein A-Sepharose beads was added to the incubation mix for an additional 1 h at 4°C. Beads were pelleted, washed thoroughly in lysis buffer, and incubated in Laemmli sample buffer at 60°C for 30 min. Bound proteins were separated using SDS-PAGE, which was followed by Western blot analysis as described earlier using either rabbit anti-α_{1C}-primary antibody at a 1:200 dilution or goat anti-biotin antibody (Abcam; Cambridge, MA) at a 1:20,000 dilution.

Whole cell electrophysiology. Coverslips with HEK-293 cells were placed in the bottom of the perfusion chamber (Warner Instruments; Hamden, CT), and transfected cells that expressed green fluorescent protein were detected by epifluorescence microscopy. Experiments were performed at 22–24°C. The ruptured whole cell pipette solution consisted of (in mM) 114 CsCl, 10 EGTA, 10 HEPES, and 5 MgATP (pH 7.2 with CsOH). Cells were initially bathed in Ca^{2+}-Tyrode solution that contained (in mM) 1.8 $CaCl_2$, 142 NaCl, 5.4 KCl, 1.0 $MgCl_2$, 0.33 Na_2H-PO_4, and 5 HEPES (pH 7.40 with NaOH). After a gigaseal was formed and the whole cell ruptured configuration was obtained, the cells were bathed in a solution that consisted of (in mM) 10 $BaCl_2$, 133 CsCl, and 10 HEPES (pH 7.4 with CsOH). For perforated patch experiments, the pipette solution consisted of 100 mM Cs-glutamine, 0.5 mM $CaCl_2$, 40 CsCl, 10 HEPES, and 60 ng of amphotericin B (pH 7.2 with CsOH). The bath solution was the same as that used for the ruptured patch configuration. The Ca^{2+} channel activator SDZ+202-791 (1 μM; Biomol Research Laboratories; Plymouth Meeting, PA) in bath solution was tested in some experiments. Whole cell currents were recorded using an Axopatch 200B amplifier (Axon Instruments; Foster City, CA). Data were sampled at 25 kHz and filtered at 5 kHz. The holding potential was −80 mV. Liquid junction potential was determined to be −3.4 mV under these conditions, and data were not corrected for this offset. Electrodes were pulled using a micropipette puller (Sutter Instruments; Novato, CA) and heat polished to obtain resistances of between 1.5 and 3.5 MΩ when filled with internal solution. Data analysis was performed using pClamp (Axon Instruments) and Origin (Microcal; Northampton, MA) software. Whole cell conductance (G) was calculated from peak current divided by the driving force, which is determined by the test potential minus the reversal potential. The reversal potential used for these calculations was +60 mV. The whole cell conductance-voltage (G-V) curve was plotted and fit by a Boltzmann function using the equation

$$\frac{G}{G_{max}} = \frac{1}{(1 + e^{-(V-V_{1/2})/k})}$$

where G_{max} is the maximum whole cell conductance, V is the potential, $V_{1/2}$ is the potential at which half-activation occurs, and k is the slope value.

Single-channel electrophysiology. Single-channel data were collected using the cell-attached patch configuration with an Axopatch 200B amplifier. Borosilicate glass electrodes were pulled and fire polished to resistances of between 2 and 6 MΩ when filled with internal solution. Electrodes were also coated with a silicone elastomer for additional noise reduction (Sylgard; Dow Corning; Midland, MI). The bath solution consisted of (in mM) 110 potassium aspartate, 30 KCl, 3.8 $MgCl_2$, 5 HEPES, 5 EGTA, 1.2 $CaCl_2$, and 10 dextrose. The Ca^{2+} channel activator SDZ+202-791 (1 μM) was included in the bath solution. The pipette solution was composed of (in mM) 100 $BaCl_2$, 20 tetraethylammonium chloride, and 10 HEPES. Junction potential was calculated to be approximately −9.3 mV for these solutions, and test potentials were corrected accordingly. Data were sampled at 10 kHz and filtered at 1–2 kHz. Data were analyzed with a custom program that used Microcal Origin. To determine mean open probability (P_o), the data were converted into idealized events using traces corrected for capacity transients and leak current by subtracting the averages of traces without openings. Channel-open events were identified by a half-height criterion.

Statistics. All values are presented as means ± SE. Statistical comparisons were made by use of the two-tailed Student's t-test. Differences with $P < 0.05$ were considered statistically significant.

RESULTS

Identification of β_{1d}-protein in heart. Our previous study identified the mRNA encoding $Ca_v\beta_{1d}$ protein in canine and human hearts (20), but the presence of the encoded protein in heart was not determined. To probe for $Ca_v\beta_{1d}$ protein expression, we produced a specific rabbit polyclonal antibody directed against the unique carboxyl terminus of $Ca_v\beta_{1d}$ that results from the alternative splicing and frame shift in this isoform. Western blot analysis of membranes from HEK-293 cells transfected with $Ca_v\beta_{1a}$, $Ca_v\beta_{1b}$, or $Ca_v\beta_{1d}$ demonstrated that the $Ca_v\beta_{1d}$ antibody recognized a 23-kDa protein only in the $Ca_v\beta_{1d}$-transfected cells of the

predicted molecular mass of 23 kDa (Fig. 2). The specificity of this antibody was highlighted by the fact that no significant immunoreactivity was found in the membranes from $Ca_v\beta_{1a}$- or $Ca_v\beta_{1b}$-transfected cells despite the amino acid sequence of $Ca_v\beta_{1d}$ protein being identical to the first six exons of $Ca_v\beta_{1a}$ and $Ca_v\beta_{1b}$ (except for the final seven amino acids, which are found uniquely in $Ca_v\beta_{1d}$). Next, the presence of $Ca_v\beta_{1d}$ protein in cardiac muscle was tested using Western blot analysis of canine and human ventricular membranes. Canine left ventricular membranes were prepared using a discontinuous sucrose gradient that isolated membrane fractions enriched in the surface sarcolemma (F1), T-tubular sarcolemma (F2), and junctional complexes (F3). The $Ca_v\beta_{1d}$ antibody readily detected a 23-kDa protein in all three canine ventricular membrane fractions that was enriched in the membrane fractions relative to crude homogenate (band seen with longer exposure; data not shown). Likewise, a 23-kDa band was detected in enriched membranes (pooled F1, F2, and F3) from human ventricle. These results demonstrate the expression of $Ca_v\beta_{1d}$ subunit at the protein level in canine and human hearts.

Membrane trafficking of α_{1C}-channels by β_{1b}- and β_{1d}-subunits. An important property of full-length $Ca_v\beta$ subunits is to promote membrane trafficking of high-voltage activated Ca^{2+} channel α_1-subunits to the surface membrane (4, 13, 27, 29). The β-interaction domain (BID) region in domain 4 of the $Ca_v\beta$ subunit has been suggested (4) to be essential to alleviate ER retention of the α_1-subunits, and more recent structural experiments have identified the ABP that lies distal to the BID in domain 4 as the region of the $Ca_v\beta$ that binds to the α-interaction domain (AID) of α_1-subunits. Therefore, we predicted that a fundamental difference between short and full-length $Ca_v\beta$ subunits would be the ability to chaperone α_1-subunits to the surface membrane. HEK-293 cells were transfected with α_{1C}-subunit alone or in combination with a representative full-length $Ca_v\beta_1$ subunit, $Ca_v\beta_{1b}$, or the short $Ca_v\beta_{1d}$. Immunolabeling was performed on transiently transfected HEK-293 cells using a rabbit polyclonal antibody to α_{1C}-subunit (16). Confocal microscopy was used to image immunolabeled cells that expressed α_{1C}-subunits alone (Fig. 3, *A* and *B*), α_{1C} + $Ca_v\beta_{1b}$ subunits (Fig. 3, *C* and *D*), and α_{1C} + $Ca_v\beta_{1d}$ subunits (Fig. 3, *E* and *F*). Comparison of the phase-contrast images (Fig. 3, *left*) with the fluorescence images (Fig. 3, *right*) of the cells demonstrates that similar immunolabeling of α_{1C}-subunits was observed for α_{1C}-subunits alone and α_{1C} + $Ca_v\beta_{1d}$-expressing cells with predominately an intracellular reticulate pattern with strong perinuclear labeling consistent with localization to the ER-Golgi system. Careful inspection of Fig. 3*D* demonstrates that α_{1C}-protein coexpressed with $Ca_v\beta_{1b}$ again shows intracellular immunofluorescence, but there is also clear membrane localization of α_{1C}-subunits as indicated by the arrows. The specificity of the immunofluorescence is demonstrated by the minimal fluorescence in a third cell (Fig. 3, *A* and *B*) that was not transfected. These results suggest that $Ca_v\beta_{1d}$ does not effectively promote membrane trafficking of α_{1C}-subunits to the surface membrane in contrast with full-length $Ca_v\beta_{1b}$.

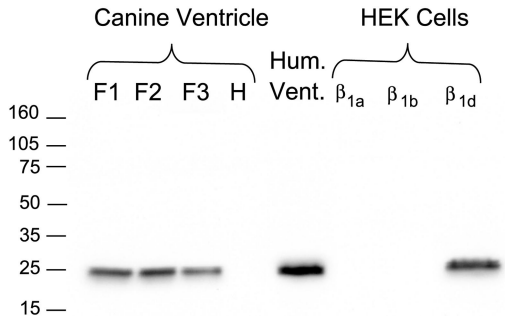

Fig. 2. Specific detection of $Ca_v\beta_{1d}$ protein in canine heart, human heart, and transfected HEK-293 cells. Western blot analysis was performed using anti-$Ca_v\beta_{1d}$ antibody on canine membrane fractions (F) enriched in surface sarcolemma (F1), T-tubular sarcolemma (F2), junctional complexes (F3), and crude membrane homogenate (H). A sample of enriched membranes from human ventricle was also tested (middle lane). Membrane homogenates from HEK-293 cells transfected with $Ca_v\beta_{1a}$, $Ca_v\beta_{1b}$, or $Ca_v\beta_{1d}$ were evaluated (right three lanes). Amount of membrane protein loaded in each lane was 60 μg.

To confirm the immunocytochemistry experiments, biotinylation experiments were performed in intact cells to detect surface membrane α_{1C}-channels in the absence and presence of $Ca_v\beta$-subunit coexpression. Intact HEK-293 cells expressing α_{1C}-subunit alone, α_{1C} + $Ca_v\beta_{1b}$, and α_{1C} + $Ca_v\beta_{1d}$ and mock transfected cells were surface biotinylated, and the whole cell lysates were immunoprecipitated using anti-α_{1C}-antibody and subsequent Western blot analysis of the immunoprecipitates. A representative Western blot (Fig. 4*A*) probed with anti-biotin antibody demonstrates a band at 240 kDa seen most prominently with $Ca_v\beta_{1b}$ coexpression relative to α_{1C}-subunits alone or α_{1C} + $Ca_v\beta_{1d}$. When the blot was stripped and reprobed with anti-α_{1C}-antibody, the same 240-kDa protein was detected, which demonstrates that the biotinylated protein was the α_{1C}-subunit. The greater signal on the anti-biotin blot for the α_{1C} + $Ca_v\beta_{1b}$ lane relative to α_{1C} and α_{1C} + $Ca_v\beta_{1d}$ suggests that $Ca_v\beta_{1b}$-subunit coexpression leads to the greatest surface membrane expression of α_{1C}-subunits. Interestingly, the anti-α_{1C}-antibody blot showed the greatest signal in the α_{1C} + $Ca_v\beta_{1b}$ lane; it showed a greater abundance of α_{1C}-subunits in the immunoprecipitates despite identical transfection and an identical protein amount loaded onto gels. Therefore, coexpression of $Ca_v\beta_{1b}$ may also stabilize the heterologously expressed α_{1C}-subunit and lead to a greater steady-state amount. In addition, other proteins were recognized with the anti-biotin blots that are associated with α_{1C}-subunits, but their identities are not known. The specificity of the findings is demonstrated by lanes for mock-transfected cells that showed no signal for anti-biotin or anti-α_{1C}-antibodies. These results were typical of five experiments. Overall, the biotinylation experiments demonstrate a greater expression of surface membrane α_{1C}-subunits when $Ca_v\beta_{1b}$ is coexpressed compared with $Ca_v\beta_{1d}$ coexpression or α_{1C}-subunit expression alone.

Effects of β_{1b}- and β_{1d}-subunits on whole cell electrophysiology of α_{1C}-channels. To directly compare the functional modulation of α_{1C}-channels by the full-length $Ca_v\beta_{1b}$ to the short $Ca_v\beta_{1d}$ subunits, transfected HEK-293 cells were studied using the whole cell configuration of the patch-clamp technique. From a holding potential of −80 mV, a series of 50-ms depolarizing pulses was applied from −50 to +80 mV in 10-mV steps, and representative raw current traces at

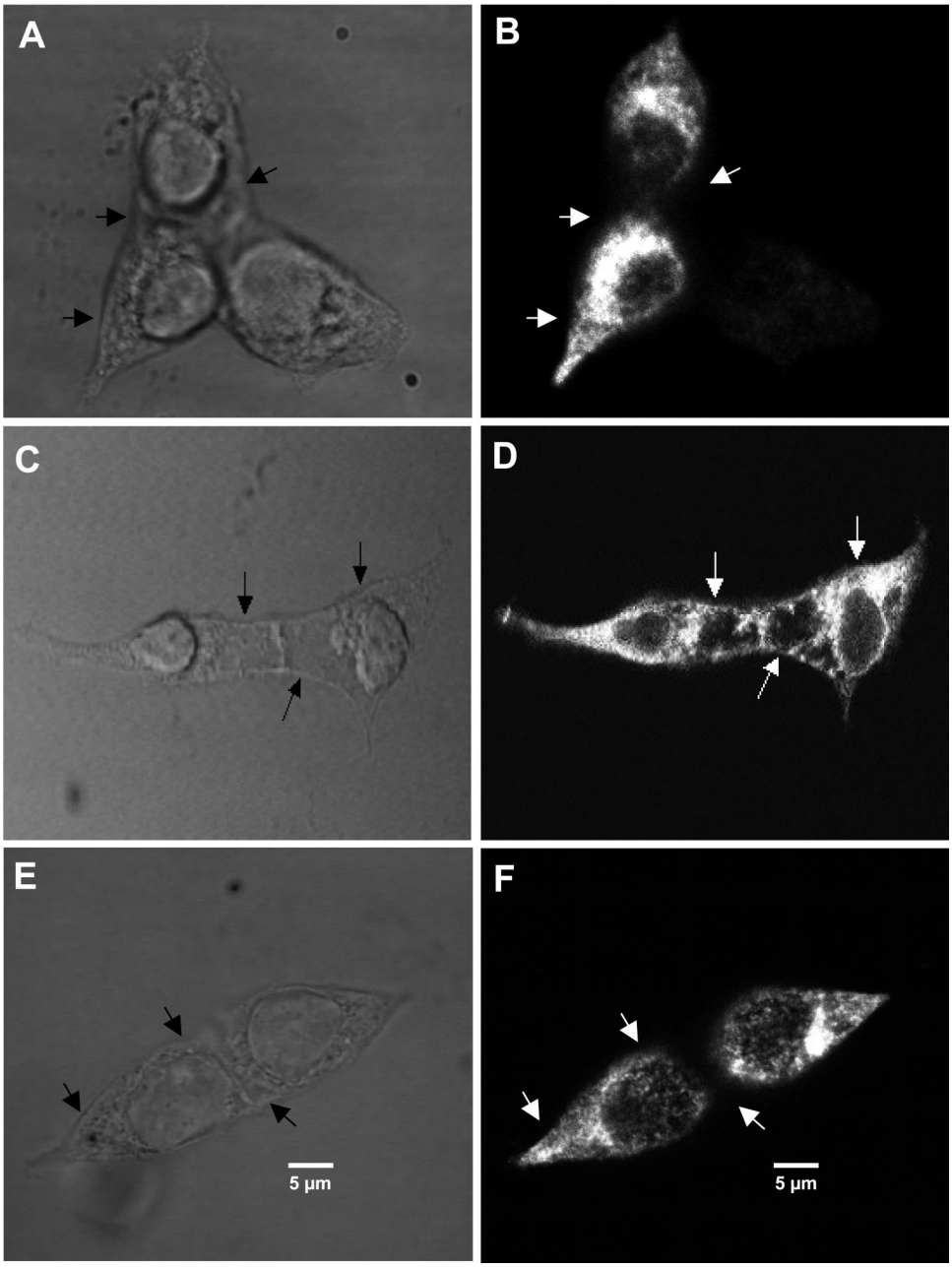

Fig. 3. $Ca_v\beta_{1b}$ but not $Ca_v\beta_{1d}$ promotes membrane trafficking of α_{1C}-subunits to surface membrane. Confocal images of HEK-293 cells transfected with α_{1c}-subunits alone (*A* and *B*), α_{1c} + β_{1b} (*C* and *D*), and α_{1C} + β_{1d} (*E* and *F*) subunits immunolabeled with an α_{1C}-antibody are shown. Phase-contrast images (*left*) of the cells and matched immunofluorescence using an Alexa Fluor 568 anti-rabbit secondary antibody (*right*) are shown. Cell surface membranes were determined by phase-contrast confocal images (arrows).

−30, −10, and +10 mV are shown in Fig. 4*A* for all subunit combinations. Expression of the Ca^{2+} channel α_{1C}-subunit alone in HEK-293 cells resulted in small inward currents carried by 10 mM Ba^{2+} that were typical of our previous studies and those of others using this expression system (21, 29, 36). The α_{1C}-currents activate in a voltage-dependent fashion, and the resulting current-voltage (*I-V)* curve (Fig. 5*B*) is bell shaped, which is characteristic of L-type Ca^{2+} channels. As anticipated, coexpression of the full-length $Ca_v\beta_{1b}$ with α_{1C}-subunits resulted in markedly greater current densities that were ~15-fold larger at the peak of the *I-V* curve compared with α_{1C}-subunits alone (coexpression, −96.4 ± 14.2, n = 11; α_{1C} alone, −6.4 ± 1.2 pA/pF, n = 6; Fig. 5). In contrast with the striking effect of $Ca_v\beta_{1b}$ on current density, coexpression of $Ca_v\beta_{1d}$ with α_{1C}-subunits did not result in a significant change in the measured currents compared with expression of α_{1C}-subunits alone (current at peak of *I-V* curve for α_{1C} + $Ca_v\beta_{1d}$, −6.69 ± 1.02 pA/pF, n = 14).

Closer inspection of the *I-V* curves suggested that coexpression of $Ca_v\beta_{1b}$ resulted in a hyperpolarizing shift in the voltage dependence of channel activation that was comparable to previous studies with this subunit and many other auxiliary $Ca_v\beta$ subunits (8, 9, 17, 21, 37). To more directly assess the impact of $Ca_v\beta$-subunit coexpression on the voltage dependence of current activation, we plotted *G* calculated from peak current vs. test potential (*V*; see MATERIALS AND METHODS). Normalized *G-V* curves are shown

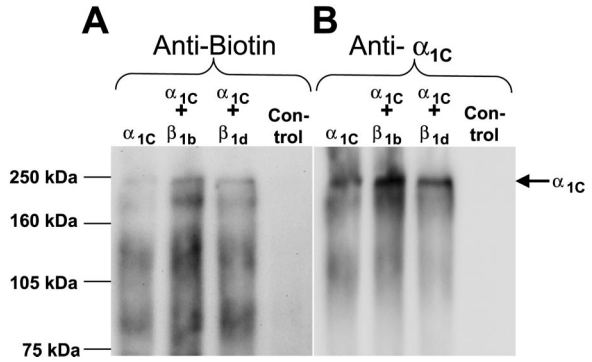

Fig. 4. Surface labeling of α_{1C}-channels through biotinylation. Cell surface biotinylation of α_{1C}-channels was examined using HEK-293 cells transiently transfected with α_{1C}-, α_{1C} + $Ca_v\beta_{1b}$, or α_{1C} + $Ca_v\beta_{1d}$ subunits. Biotin-labeled HEK-293 cell lysate was immunoprecipitated with anti-α_{1C}-antibody and subjected to Western blot analysis with anti-biotin antibody (*A*) then stripped and reprobed with anti-α_{1C}-antibody (*B*); the 240-kDa α_{1C}-subunit is indicated.

for α_{1C}-, α_{1C} + β_{1b}-, and α_{1C} + β_{1d}-subunit combinations in Fig. 5*C*, and the data were fit to Boltzmann distributions that resulted in $V_{1/2}$ values of -3.9 ± 0.8, -10.2 ± 1.7, and -5.0 ± 1.1 mV, respectively; and for k values of 7.4 ± 0.6, 4.2 ± 1.7, and 6.6 ± 0.9 mV, respectively. These data demonstrate that coexpression of $Ca_v\beta_{1b}$ with the α_{1C}-subunit results in a 6.3-mV hyperpolarizing shift in the $V_{1/2}$ for current activation with a steeper activation curve, but coexpression of $Ca_v\beta_{1d}$ has no significant effect on the voltage dependence of current activation.

Another prominent and well-characterized effect of $Ca_v\beta$ subunits is to modulate the kinetics of current decay or inactivation (12, 34, 36, 49). From a holding potential of -80 mV, 250-ms voltage steps were given to -20, -10, 0, 10, and 20 mV. Current inactivation was measured as the fraction of current remaining at 50 ms (r50) and 200 ms (r200) relative to the peak current. Representative normalized current traces at $+10$ mV for each subunit combination are plotted in Fig. 6*A*, and average data over the range of membrane potentials for r50 and r200 are shown in Fig. 6, *B* and *C*. There was no significant difference between α_{1C}-subunits alone and α_{1C} + $Ca_v\beta_{1d}$ in current decay at any potential measured for r50 and r200. However, coexpression of $Ca_v\beta_{1b}$ significantly accelerated current decay at positive potentials as can be seen in both the r50 and r200 measurements.

$Ca_v\beta_{1b}$ and $Ca_v\beta_{1d}$ subunits modulate single-channel properties of α_{1C}-channels. Our experiments to this point demonstrate that $Ca_v\beta_{1d}$ is expressed as a protein in transfected HEK-293 cells, but no effects were detected on the whole cell currents with $Ca_v\beta_{1d}$ expression, which is in sharp contrast to the marked effects of $Ca_v\beta_{1b}$ coexpression. We decided to

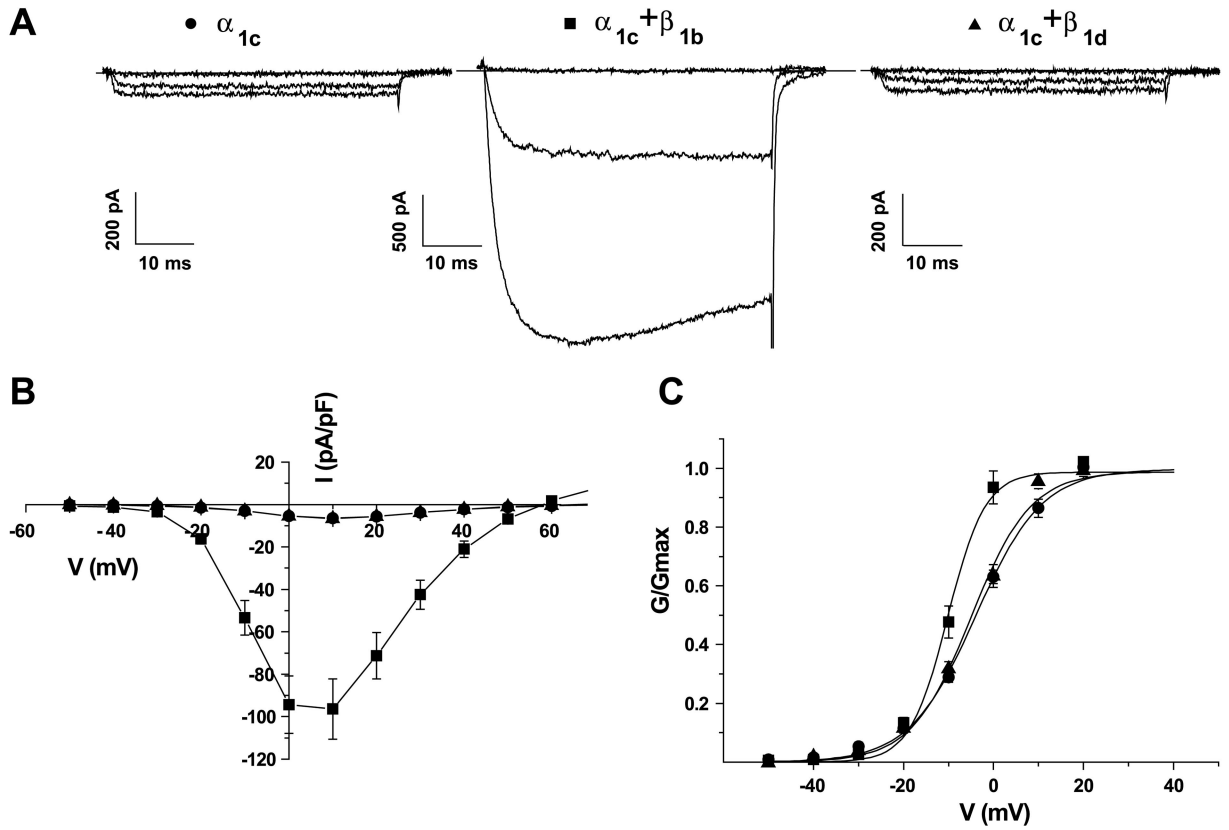

Fig. 5. Effects of $Ca_v\beta_{1b}$ and $Ca_v\beta_{1d}$ coexpression on α_{1C}-whole cell Ba^{2+} current (I_{Ba}) in transiently transfected HEK-293 cells. Whole cell I_{Ba} was measured from HEK-293 cells transfected with α_{1C}-subunits alone, α_{1C} + β_{1b}, or α_{1C} + β_{1d} subunits. Cells were held at -80 mV and given a series of 50-ms pulses from -50 to $+80$ mV. Representative raw current traces (test potentials of -30, -10, and $+10$ mV) are shown (*A*). Average I_{Ba}-voltage (*V*) data were normalized to cell capacitance (*B*). Normalized whole cell conductance (G/G_{max}) is plotted vs. voltage (*C*). Average data were fit to Boltzmann distributions.

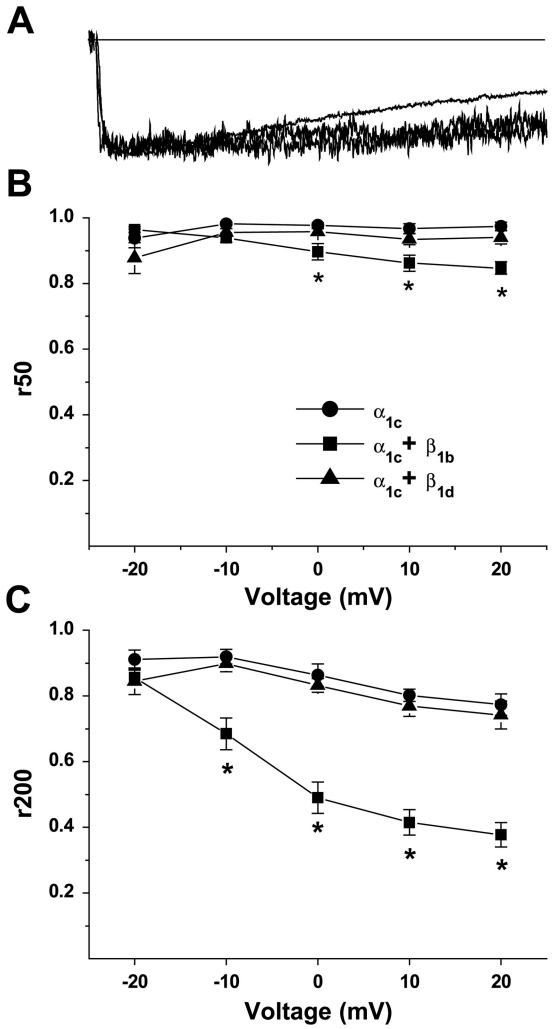

Fig. 6. $Ca_v\beta_{1b}$ but not $Ca_v\beta_{1d}$ increases rate of I_{Ba} inactivation. I_{Ba} decay at +10 mV was compared for cells expressing α_{1C}-subunits alone, α_{1C} + β_{1b}, and α_{1d} + β_{1b} subunits. Representative normalized raw current traces at +10 mV are plotted (*A*). Average data comparing ratio of I_{Ba} remaining at 50 ms (r50; *B*) or 200 ms (r200; *C*) relative to peak I_{Ba} for different Ca^{2+} channel subunit combinations (n = 5, 10, and 10 for α_{1C}-subunits alone, α_{1C} + β_{1b}, and α_{1C} + β_{1d}, respectively; *$P < 0.05$ relative to α_{1C}-subunits only).

examine single-channel currents in the transfected HEK-293 cells, because Hullin et al. (26) recently showed that there was no measurable effect of another short $Ca_v\beta$ subunit, $Ca_v\beta_{3d}$, when it was coexpressed with α_{1C}-subunits in whole cell recordings, but modulation was revealed by single-channel studies.

Transiently transfected HEK-293 cells were studied with the cell-attached patch-clamp technique to measure single-channel currents. Cells were transfected with the α_{1C}-subunit with or without auxiliary $Ca_v\beta_1$ subunits. In these experiments, truncated amino-terminal subunits (deletion of first 13 amino acids), $Ca_v\beta_{1b}\Delta$1-13 and $Ca_v\beta_{1d}\Delta$1-13, were studied in an effort to begin determination of the essential amino acids for modulation of the α_{1C}-currents. Whole cell studies of expressed $Ca_v\beta_{1b}\Delta$1-13 and $Ca_v\beta_{1d}\Delta$1-13 showed indistinguishable modulation of the whole cell currents relative to the nontruncated $Ca_v\beta_{1b}$- and $Ca_v\beta_{1d}$-subunits (data not shown). Single-channel studies were done in the presence of the Ca^{2+} channel activator SDZ+202-791 to stimulate single-channel activity and produce longer openings and thereby allow more accurate measurement of single-channel currents. Patches were held at −80 mV and given test pulses to −10 mV for 200 ms. Figure 7 shows representative current traces from multichannel patches with the different subunit combinations. Under our experimental conditions, patches containing only a single channel were never observed when $Ca_v\beta$ subunits were coexpressed. Inspection of the representative currents shows sparse openings with many null sweeps for the patches expressing α_{1C}-subunits alone but greater channel activity in the patches coexpressing the auxiliary $Ca_v\beta_{1b}\Delta$1-13 and $Ca_v\beta_{1d}\Delta$1-13 subunits. Openings were typically long lived, which is as expected from the presence of SDZ+202-791. Ensemble average currents in Fig. 7*B* suggest that average currents were increased by coexpression of $Ca_v\beta_{1b}$ or $Ca_v\beta_{1d}$ subunits.

In general terms, the apparent greater single-channel activity observed with $Ca_v\beta_1$-subunit coexpression could be due to changes in channel number in the patches and/or alterations in channel gating. Therefore, we sought to first measure channel number in each patch. By taking advantage of the presence of a Ca^{2+} channel activator and using a strong depolarization protocol to facilitate channel openings, we measured the number of stacked openings as an index of channel number as shown in Fig. 8*A*. As seen in Fig. 8*B*, the average number of channels detected per patch was significantly increased approximately eightfold by $Ca_v\beta_{1b}\Delta$1-13 coexpression, whereas expression of $Ca_v\beta_{1d}\Delta$1-13 did not significantly change the number of channels observed per patch compared with α_{1C}-subunits alone.

Next we assessed the effect of $Ca_v\beta$ subunit coexpression on average single-channel gating by determining the mean P_o for each subunit combination by correcting for the channel number. In Fig. 9*A*, mean P_o is significantly increased by coexpression of either $Ca_v\beta_{1b}\Delta$1-13 or $Ca_v\beta_{1d}\Delta$1-13. Both subunits comparably increased P_o in the range of fourfold. This observation provides the strongest evidence that the short $Ca_v\beta_{1d}$ subunit can interact with the α_{1C}-channel and modulate single-channel gating. Although coexpression of $Ca_v\beta_1$ subunits altered single-channel gating, they did not alter the single-channel conductance (g) of the expressed channels (α_{1C}-subunits alone, 27.1 ± 0.1; α_{1C} + $Ca_v\beta_{1d}\Delta$1-13, 28.0 ± 0.1; and α_{1C} + $Ca_v\beta_{1b}\Delta$1-13, 26.3 ± 0.3 pS) as shown in Fig. 9*B*.

To determine whether the similar single-channel gating behavior of $Ca_v\beta_{1b}\Delta$1-13- and $Ca_v\beta_{1d}\Delta$1-13-coexpressing channels was due to intrinsically similar modulatory properties of the subunits or was confounded by differential sensitivity to SDZ+202-791, we directly measured the effect of 1 μM SDZ+202-791. These experiments used the perforated patch technique to most closely simulate conditions for single-channel recordings. Both α_{1C} + $Ca_v\beta_{1b}\Delta$1-13- and α_{1C} + $Ca_v\beta_{1d}$ Δ1-13-transfected cells showed similar increases in current (90.3 ± 12.2%, n = 5 and 83.5 ± 5.0%, n = 4, respectively). Thus the similar single-channel gating changes imparted by

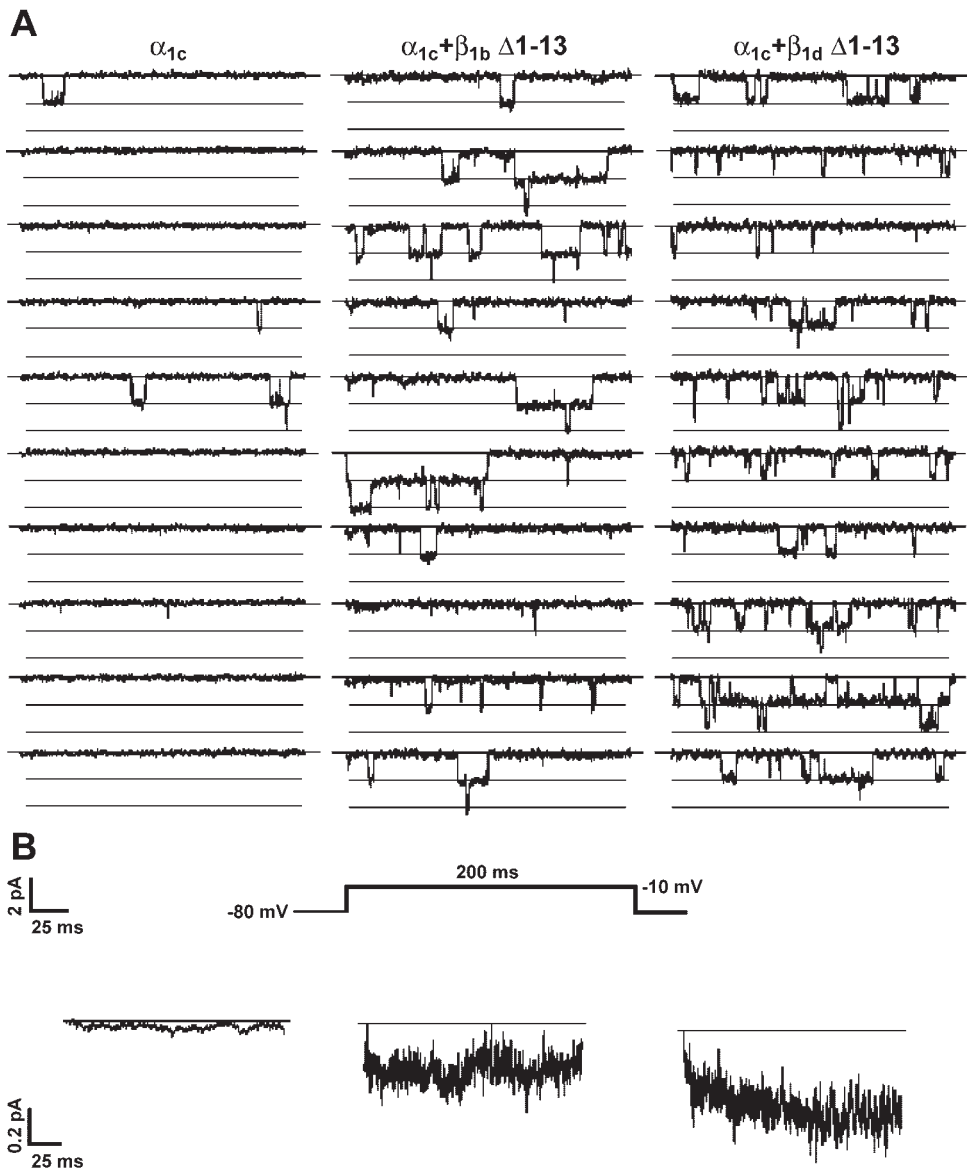

Fig. 7. $Ca_v\beta_{1b}$ and $Ca_v\beta_{1d}$ increase measured single-channel activity when coexpressed with α_{1C}-channels. HEK-293 cells transiently transfected with α_{1C}-subunits alone, α_{1C} + $Ca_v\beta_{1b}$, and α_{1C} + $Ca_v\beta_{1d}$ subunits were examined for single-channel activity using the cell-attached configuration of the patch-clamp technique with 1 μM SDZ+202-791 in the bath. Representative consecutive single-channel current traces for patches held at −80 mV that were given a 200-ms test pulse to −10 mV every 1 s are shown (*A*). Closed level (solid line), channel openings (downward deflections), and open levels (thin lines) are indicated. Ensemble average currents for each subunit combination are shown (*B*). Measured numbers of channels per patch were two for α_{1C} alone, six for α_{1C} + $Ca_v\beta_{1b}$, and seven for $Ca_v\beta_{1d}$.

$Ca_v\beta_{1b}$ or $Ca_v\beta_{1d}$ were not confounded by differences in sensitivity to SDZ+202-791.

DISCUSSION

In the present study, we demonstrate expression of the recently identified $Ca_v\beta_{1d}$ isoform as a 23-kDa protein in canine and human hearts, and we examine the functional properties of $Ca_v\beta_{1d}$ using heterologous expression studies. In contrast with the full-length splice variants of the $Ca_v\beta_1$ gene, expression of $Ca_v\beta_{1d}$, which lacks the ABP, fails to traffic α_{1C}-channels to the surface membrane. However, coexpression of the $Ca_v\beta_{1d}$ subunit can modulate the gating properties of the expressed α_{1C}-channels when examined at the single-channel level as manifest by a $Ca_v\beta_{1d}$ subunit-induced increase in mean P_o.

Lack of membrane trafficking by $Ca_v\beta_{1d}$ subunit. The ability of $Ca_v\beta$ subunits to promote trafficking of $Ca_v1.x$ and $Ca_v2.x$ channels to the surface membrane has been demonstrated in a variety of studies using techniques ranging from intramembrane charge movement to immunofluorescence assays (3, 13, 21, 27, 29). Studies have attributed this effect to the $Ca_v\beta$ subunit binding an ER retention signal localized near the AID in the I-II loop of the Ca^{2+} channel α_1-subunit (4). In particular, the BID of the $Ca_v\beta$ subunit present in domain 4 was initially found to be essential for the effect on membrane trafficking of the channel complex (4). However, more recent crystallographic studies (11, 45) suggest that the effects of mutations in the BID are related to alterations in proper protein folding, because the ABP is the actual binding site that recognizes the AID where the ER retention signal is localized. The present immunocytochemistry, surface-membrane biotinylation, and single-channel electrophysiology results demonstrating a lack of membrane trafficking by $Ca_v\beta_{1d}$ are consistent with predications that ABP binding to the AID is necessary to relieve ER retention of the α_1-subunit. Two previous studies (25, 26) have charac-

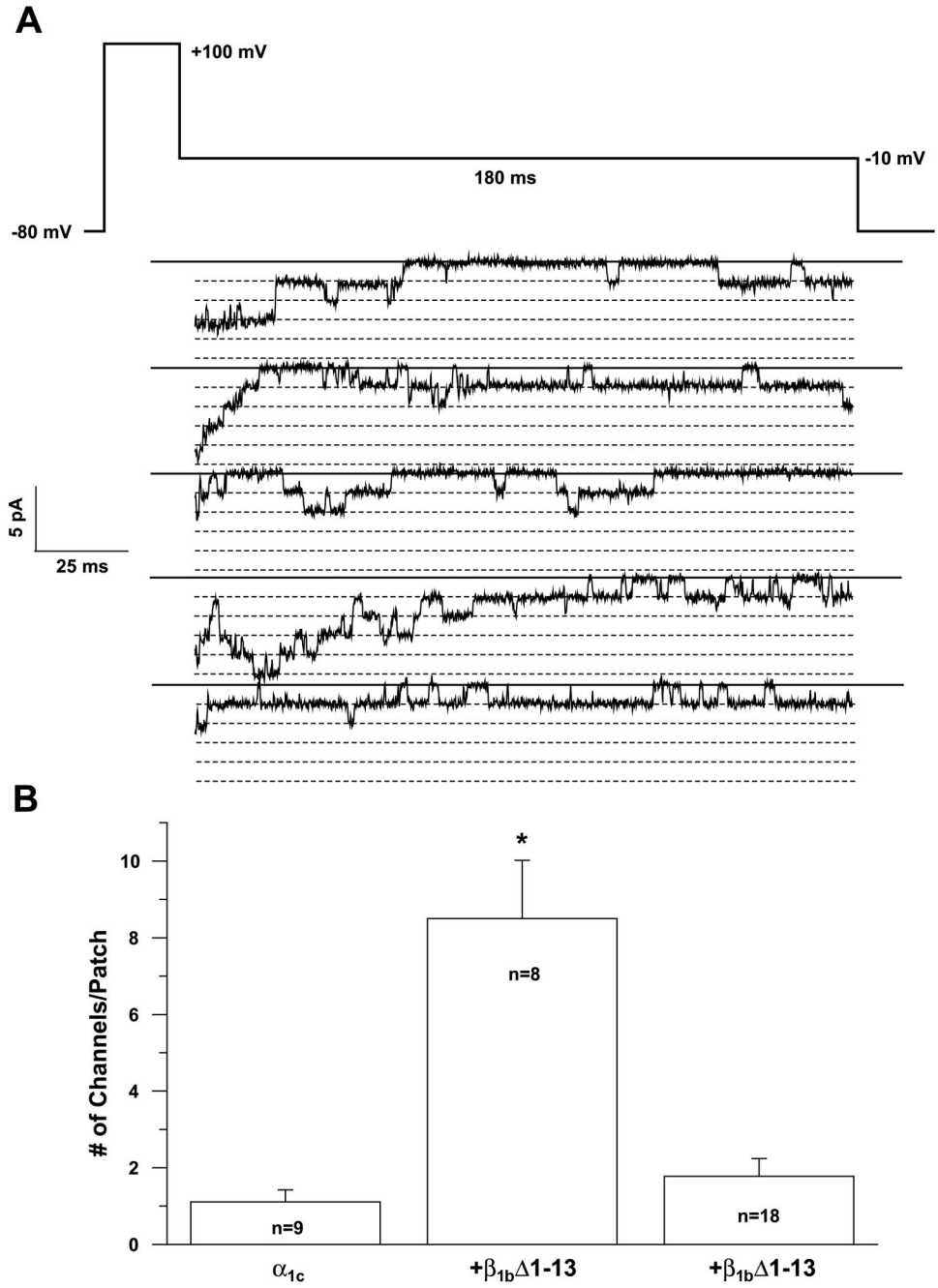

Fig. 8. Coexpression of $Ca_v\beta_{1b}$ but not $Ca_v\beta_{1d}$ increases the average number of α_{1C}-channels present in cell-attached patches. Voltage protocol and five consecutive representative single-channel traces from a cell transfected with α_{1C}- and $Ca_v\beta_{1b}$ subunits are shown (*A*). To determine the number of channels present in a given patch, experiments were done in the presence of 1 μM SDZ+202-791 and with strong facilitating depolarizations to optimize our ability to detect stacked openings. Average numbers of channels per patch for each Ca^{2+} channel subunit combination are indicated (*B*).*$P <$ 0.05, relative to α_{1C} alone and α_{1C} + β_{1d}.

terized functional effects of other short $Ca_v\beta$-splice variants including truncated splice variants of the $Ca_v\beta_3$ and $Ca_v\beta_4$ genes, but those studies did not directly address membrane trafficking. It is likely that all short $Ca_v\beta$ subunits will share the inability to promote membrane trafficking given the lack of the ABP.

A number of different signaling pathways affect the trafficking of Ca^{2+} channels to the surface membrane by interacting with $Ca_v\beta$ subunits. For example, the Ras-related small G protein Gem/Kir can markedly downregulate the surface expression of $Ca_v1.3$ L-type Ca^{2+} channels in endocrine cells (2). Other related proteins in this family including the Rem and Rad GTPases share the ability to remarkably reduce if not eliminate expressed Ca^{2+} channel activity in a $Ca_v\beta$-subunit-dependent manner (19). In addition, neuronal Ca^{2+} sensor-1 (NCS-1) can also downregulate the expression of voltage-gated Ca^{2+} channels in a $Ca_v\beta$-subunit-specific fashion (39). However, the effects of NCS-1 on Ca^{2+} currents have varied among different experimental systems with some studies showing that NCS facilitates or increases P/Q- and N-type Ca^{2+} currents, which may be important for activity-dependent synaptic facilitation or synaptic neurotrophic effects (44, 48). Ultimately, understanding how these accessory proteins modulate channel expression and function will require more detailed understanding of how they interact with $Ca_v\beta$

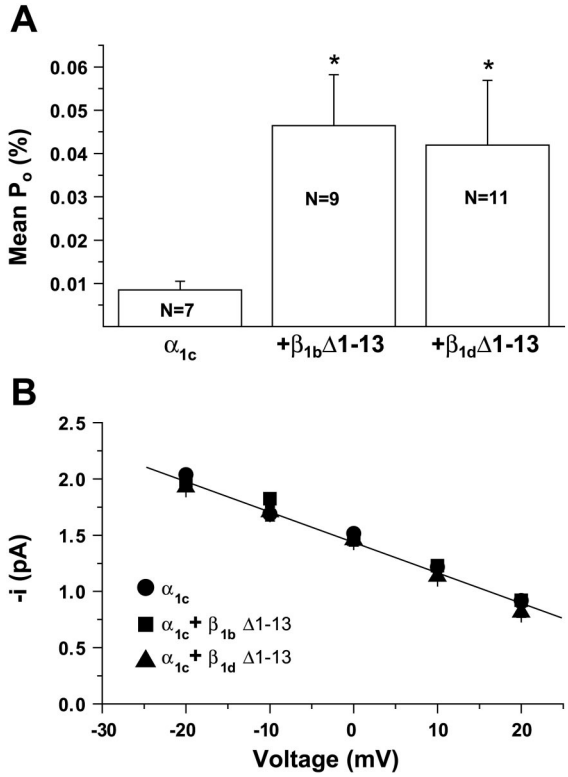

Fig. 9. Comparison of mean open probability (P_o) and single-channel conductance for α_{1C}-channels alone or with $Ca_v\beta_{1b}$ or $Ca_v\beta_{1d}$. Calculated mean P_o values are shown for each Ca^{2+} channel subunit combination after correction for the number of channels present at a test potential of −10 mV (*A*). $*P <$ 0.05 compared with α_{1C}-subunits alone. Single-channel current is plotted as a function of test voltage for α_{1C}-, α_{1C} + $Ca_v\beta_{1b}$-, and α_{1C} + $Ca_v\beta_{1d}$-expressing cells (*B*). Linear regression fit of α_{1C}-subunit data is displayed. Single-channel conductance (*g*) was calculated from the slope of the fit lines for each subunit combination (α_{1C}, 27.1 ± 0.1; α_{1C} + $Ca_v\beta_{1b}$, 26.3 ± 0.03; and α_{1C} + $Ca_v\beta_{1d}$, 28.0 ± 0.1 pS). There were no significant differences among groups for single-channel conductance.

subunits including determining what region of the $Ca_v\beta$ subunit is required for these effects, how different $Ca_v\beta$ subunits vary in response, and in particular, whether the short $Ca_v\beta$ subunits such as $Ca_v\beta_{1d}$ are capable of modulating this process perhaps by binding to the regulatory proteins without affecting the trafficking of the channels. Therefore, although the short $Ca_v\beta$ subunits may not directly affect membrane trafficking of the channel complex, they may act as a sink for modulatory molecules binding to $Ca_v\beta$ subunits that could affect trafficking.

Functional effects of short $Ca_v\beta$ subunits on Ca^{2+} channel gating. Although our data suggest that $Ca_v\beta_{1d}$ has no detectable effect on membrane trafficking of the α_{1C}-complex, we provide evidence that the $Ca_v\beta_{1d}$ subunit can still modulate the gating of the channels by increasing the mean P_o. Comparably, a recent study (26) examining the effect of coexpression of a truncated $Ca_v\beta_3$ subunit lacking the ABP with α_{1C}-subunits also demonstrated an increase in single-channel activity. These results demonstrate that it is possible to separate the effects of the $Ca_v\beta$ subunit on membrane trafficking from its ability to modulate channel gating. Even with full-length $Ca_v\beta$ subunits, a previous study (21) has shown that the major functional effects of $Ca_v\beta$ subunits can be separated from membrane-trafficking effects by mutating a critical residue in the AID in the domain I-II loop of α_{1C}-subunits. In that heterologous expression study, $Ca_v\beta$-subunit coexpression failed to traffic the AID mutated α_{1C}-subunit to the surface membrane, but the $Ca_v\beta$ subunit was clearly able to modulate single-channel gating (21). In addition, in another study (51) in which $Ca_v\beta_3$ fusion proteins were injected into oocytes, the investigators showed that alterations in channel gating occurred much more rapidly than the effects on membrane trafficking. These authors likewise concluded that channel-gating and membrane-trafficking effects could be separately controlled by $Ca_v\beta$ subunits.

The modulation of gating of α_{1C}-channels by the short $Ca_v\beta_{1d}$ subunit suggests that sites of interaction between α_{1C}- and $Ca_v\beta_{1d}$ subunits exist besides the well-characterized binding of α_{1C}-AID in the I-II linker to the $Ca_v\beta$ ABP in domain 4. Previous studies (46, 47) have described interactions between the carboxyl terminus of $Ca_v\beta_4$ and both the amino and carboxyl termini of the $Ca_v2.1$ channel. These interactions, which do not involve the AID and ABP, have generally been found to be of much lower affinity. Additionally, others have argued that the association of the $Ca_v\beta$ subunits with α_{1C}-channels is dynamic and reversible, so multiple low-affinity sites may allow for specific modulation (5, 38). Our data with the short $Ca_v\beta_{1d}$ subunit provide evidence for an uncharacterized interaction site that occurs in the amino terminal half rather than the carboxyl terminal portion of the $Ca_v\beta_1$ subunit. Furthermore, the interaction site does not involve the first 13 amino acid residues of $Ca_v\beta_1$. Lower affinity interactions by the short $Ca_v\beta$ subunits may also help to explain the apparent discrepancy between the lack of whole cell electrophysiology effects and the increase in mean P_o observed in single-channel measurements observed in our study and that of Hullin et al. (26).

The functional impact of short $Ca_v\beta$ subunits such as $Ca_v\beta_{1d}$ in cell physiology may also be related to their ability to interact with other $Ca_v\beta$ subunits or even other proteins independent of the channel complex. The modular $Ca_v\beta$ subunit, like other MAGUKs, can undergo intermolecular interactions that involve SH3 and GK domains (32, 42). Therefore, it is possible that short $Ca_v\beta$ subunits interact with full-length $Ca_v\beta$ subunits to ultimately affect channel gating and trafficking. In addition, the recently described (25) regulation of gene expression by short splice variants of the $Ca_v\beta_4$ gene provides evidence for other important roles of these proteins. Future studies are needed to define the full array of functional interactions of short $Ca_v\beta$ subunits in cell physiology.

ACKNOWLEDGMENTS

The authors acknowledge the assistance of Thankful Sanftleben with manuscript preparation.

GRANTS

This study was supported by National Institutes of Health Grants R01 HL-61537 (to T. J. Kamp) and PO1 HL-47053 (to T. J. Kamp and J. W. Hell).

REFERENCES

1. **Balijepalli RC, Lokuta AJ, Maertz NA, Buck JM, Haworth RA, Valdivia HH, and Kamp TJ.** Depletion of t-tubules and specific subcellular changes in sarcolemmal proteins in tachycardia-induced heart failure. *Cardiovasc Res* 59: 67–77, 2003.
2. **Beguin P, Nagashima K, Gonoi T, Shibasaki T, Takahashi K, Kashima Y, Ozaki N, Geering K, Iwanaga T, and Seino S.** Regulation of Ca^{2+} channel expression at the cell surface by the small G-protein kir/Gem. *Nature* 411: 701–706, 2001.
3. **Beurg M, Sukhareva M, Strube C, Powers PA, Gregg RG, and Coronado R.** Recovery of Ca^{2+} current, charge movements, and Ca^{2+} transients in myotubes deficient in dihydropyridine receptor beta 1 subunit transfected with beta 1 cDNA. *Biophys J* 73: 807–818, 1997.
4. **Bichet D, Cornet V, Geib S, Carlier E, Volsen S, Hoshi T, Mori Y, and de Waard M.** The I-II loop of the Ca^{2+} channel alpha1 subunit contains an endoplasmic reticulum retention signal antagonized by the beta subunit. *Neuron* 25: 177–190, 2000.
5. **Bichet D, Lecomte C, Sabatier JM, Felix R, and de Waard M.** Reversibility of the Ca^{2+} channel $alpha_1$-beta subunit interaction. *Biochem Biophys Res Commun* 277: 729–735, 2000.
6. **Birnbaumer L, Qin N, Olcese R, Tareilus E, Platano D, Costantin J, and Stefani E.** Structures and functions of calcium channel beta subunits. *J Bioenerg Biomembr* 30: 357–375, 1998.
7. **Brice NL and Dolphin AC.** Differential plasma membrane targeting of voltage-dependent calcium channel subunits expressed in a polarized epithelial cell line. *J Physiol* 515: 685–694, 1999.
8. **Castellano A, Wei X, Birnbaumer L, and Perez-Reyes E.** Cloning and expression of a neuronal calcium channel beta subunit. *J Biol Chem* 268: 12359–12366, 1993.
9. **Castellano A, Wei X, Birnbaumer L, and Perez-Reyes E.** Cloning and expression of a third calcium channel beta subunit. *J Biol Chem* 268: 3450–3455, 1993.
10. **Catterall WA.** Structure and regulation of voltage-gated Ca^{2+} channels. *Annu Rev Cell Dev Biol* 16: 521–555, 2000.
11. **Chen YH, Li MH, Zhang Y, He LL, Yamada Y, Fitzmaurice A, Shen Y, Zhang H, Tong L, and Yang J.** Structural basis of the alpha1-beta subunit interaction of voltage-gated Ca^{2+} channels. *Nature* 429: 675–680, 2004.
12. **Chien AJ, Carr KM, Shirokov RE, Rios E, and Hosey MM.** Identification of palmitoylation sites within the L-type calcium channel $beta_{2a}$ subunit and effects on channel function. *J Biol Chem* 271: 26465–26468, 1996.
13. **Chien AJ, Zhao XL, Shirokov RE, Puri TS, Chang CF, Sun D, Rios E, and Hosey MM.** Roles of a membrane-localized beta-subunit in the formation and targeting of functional L-type Ca^{2+} channels. *J Biol Chem* 270: 30036–30044, 1995.
14. **Cohen RM, Foell JD, Balijepalli RC, Hell JW, and Kamp TJ.** Unique modulation of $Ca_{v1.2}$ channel by β_{1d} subunit (Abstract). *Biophys J* 84: 1957, 2003.
15. **Colecraft HM, Alseikhan B, Takahashi SX, Chaudhuri D, Mittman S, Yegnasubramanian V, Alvania RS, Johns DC, Marban E, and Yue DT.** Novel functional properties of Ca^{2+} channel beta subunits revealed by their expression in adult rat heart cells. *J Physiol* 541: 435–452, 2002.
16. **Davare MA, Dong F, Rubin CS, and Hell JW.** The A-kinase anchor protein MAP2B and cAMP-dependent protein kinase are associated with class C L-type calcium channels in neurons. *J Biol Chem* 274: 30280–30287, 1999.
17. **DeWaard M, Pragnell M, and Campbell KP.** Ca^{2+} channel regulation by a conserved beta-subunit domain. *Neuron* 13: 495–503, 1994.
18. **DeWaard M, Witcher DR, and Campbell KP.** Functional properties of the purified N-type Ca^{2+} channel from rabbit brain. *J Biol Chem* 269: 6716–6724, 1994.
19. **Finlin BS, Crump SM, Satin J, and Andres DA.** Regulation of voltage-gated calcium channel activity by the Rem and Rad GTPases. *Proc Natl Acad Sci USA* 100: 14469–14474, 2003.
20. **Foell JD, Balijepalli RC, Delisle BP, Yunker AM, Robia SL, Walker JW, McEnery MW, January CT, and Kamp TJ.** Molecular heterogeneity of calcium channel beta-subunits in canine and human heart: evidence for differential subcellular localization. *Physiol Genomics* 17: 183–200, 2004.
21. **Gerster U, Neuhuber B, Groschner K, Striessnig J, and Flucher BE.** Current modulation and membrane targeting of the calcium channel $alpha_{1c}$ subunit are independent functions of the beta subunit. *J Physiol* 517: 353–368, 1999.
22. **Gregg RG, Messing A, Strube C, Beurg M, Moss R, Behan M, Sukhareva M, Haynes S, Powell JA, Coronado R, and Powers PA.** Absence of the beta subunit (cchb1) of the skeletal muscle dihydropyridine receptor alters expression of the alpha 1 subunit and eliminates excitation-contraction coupling. *Proc Natl Acad Sci USA* 93: 13961–13966, 1996.
23. **Hadley RW and Lederer WJ.** Properties of L-type calcium-channel gating current in isolated guinea-pig ventricular myocytes. *J Gen Physiol* 98: 265–285, 1991.
24. **Helton TD and Horne WA.** Alternative splicing of the $beta_4$ subunit has $alpha_1$ subunit subtype-specific effects on Ca^{2+} channel gating. *J Neurosci* 22: 1573–1582, 2002.
25. **Hibino H, Pironkova R, Onwumere O, Rousset M, Charnet P, Hudspeth AJ, and Lesage F.** Direct interaction with a nuclear protein and regulation of gene silencing by a variant of the Ca^{2+}-channel beta 4 subunit. *Proc Natl Acad Sci USA* 100: 307–312, 2003.
26. **Hullin R, Khan IF, Wirtz S, Mohacsi P, Varadi G, Schwartz A, and Herzig S.** Cardiac L-type calcium channel beta-subunits expressed in human heart have differential effects on single channel characteristics. *J Biol Chem* 278: 21623–21630, 2003.
27. **Josephson IR and Varadi G.** The beta subunit increases Ca^{2+} currents and gating charge movements of human cardiac L-type Ca^{2+} channels. *Biophys J* 70: 1285–1293, 1996.
28. **Kamp TJ, Hu H, and Marban E.** Voltage-dependent facilitation of cardiac L-type Ca channels expressed in HEK-293 cells requires β-subunit. *Am J Physiol Heart Circ Physiol* 278: H126–H136, 2000.
29. **Kamp TJ, Perez-Garcia MT, and Marban E.** Enhancement of ionic current and charge movement by coexpression of calcium channel beta 1A subunit with alpha 1C subunit in a human embryonic kidney cell line. *J Physiol* 492: 89–96, 1996.
30. **Lacerda AE, Kim HS, Ruth P, Perez-Reyes E, Flockerzi V, Hofmann F, Birnbaumer L, and Brown AM.** Normalization of current kinetics by interaction between the alpha 1 and beta subunits of the skeletal muscle dihydropyridine-sensitive Ca^{2+} channel. *Nature* 352: 527–530, 1991.
31. **Laemmli UK.** Cleavage of structural proteins during the assembly of the head of bacteriophage T4. *Nature* 227: 680–685, 1970.
32. **McGee AW, Nunziato DA, Maltez JM, Prehoda KE, Pitt GS, and Bredt DS.** Calcium channel function regulated by the SH3-GK module in beta subunits. *Neuron* 42: 89–99, 2004.
33. **Mikami A, Imoto K, Tanabe T, Niidome T, Mori Y, Takeshima H, Narumiya S, and Numa S.** Primary structure and functional expression of the cardiac dihydropyridine-sensitive calcium channel. *Nature* 340: 230–233, 1989.
34. **Olcese R, Qin N, Schneider T, Neely A, Wei X, Stefani E, and Birnbaumer L.** The amino terminus of a calcium channel beta subunit sets rates of channel inactivation independently of the subunit's effect on activation. *Neuron* 13: 1433–1438, 1994.
35. **Opatowsky Y, Chen CC, Campbell KP, and Hirsch JA.** Structural analysis of the voltage-dependent calcium channel beta subunit functional core and its complex with the alpha 1 interaction domain. *Neuron* 42: 387–399, 2004.
36. **Perez-Garcia MT, Kamp TJ, and Marban E.** Functional properties of cardiac L-type calcium channels transiently expressed in HEK293 cells. Role of alpha 1 and beta subunits. *J Gen Physiol* 105: 289–305, 1995.
37. **Perez-Reyes E, Castellano A, Kim HS, Bertrand P, Baggstrom E, Lacerda AE, Wei XY, and Birnbaumer L.** Cloning and expression of a cardiac/brain beta subunit of the L-type calcium channel. *J Biol Chem* 267: 1792–1797, 1992.
38. **Restituito S, Cens T, Rousset M, and Charnet P.** Ca^{2+} channel inactivation heterogeneity reveals physiological unbinding of auxiliary beta subunits. *Biophys J* 81: 89–96, 2001.
39. **Rousset M, Cens T, Gavarini S, Jeromin A, and Charnet P.** Down-regulation of voltage-gated Ca^{2+} channels by neuronal calcium sensor-1 is beta subunit-specific. *J Biol Chem* 278: 7019–7026, 2003.
40. **Singer D, Biel M, Lotan I, Flockerzi V, Hofmann F, and Dascal N.** The roles of the subunits in the function of the calcium channel. *Science* 253: 1553–1557, 1991.
41. **Slish DF, Engle DB, Varady G, Lotan I, Singer D, Dascal N, and Schwartz A.** Evidence for the existence of a cardiac specific isoform of the α_1 subunit of the voltage-dependent calcium channel. *FEBS Lett* 250: 509–514, 1989.

42. **Takahashi SX, Miriyala J, and Colecraft HM.** Membrane-associated guanylate kinase-like properties of beta-subunits required for modulation of voltage-dependent Ca^{2+} channels. *Proc Natl Acad Sci USA* 101: 7193–7198, 2004.
43. **Takahashi SX, Mittman S, and Colecraft HM.** Distinctive modulatory effects of five human auxiliary $beta_2$ subunit splice variants on L-type calcium channel gating. *Biophys J* 84: 3007–3021, 2003.
44. **Tsujimoto T, Jeromin A, Saitoh N, Roder JC, and Takahashi T.** Neuronal calcium sensor 1 and activity-dependent facilitation of P/Q-type calcium currents at presynaptic nerve terminals. *Science* 295: 2276–2279, 2002.
45. **Van Petegem F, Clark KA, Chatelain FC, and Minor DL Jr.** Structure of a complex between a voltage-gated calcium channel beta-subunit and an alpha-subunit domain. *Nature* 429: 671–675, 2004.
46. **Walker D, Bichet D, Campbell KP, and de Waard M.** A $beta_4$ isoform-specific interaction site in the carboxyl-terminal region of the voltage-dependent Ca^{2+} channel $alpha_{1A}$ subunit. *J Biol Chem* 273: 2361–2367, 1998.
47. **Walker D, Bichet D, Geib S, Mori E, Cornet V, Snutch TP, Mori Y, and de Waard M.** A new beta subtype-specific interaction in $alpha_{1A}$ subunit controls P/Q-type Ca^{2+} channel activation. *J Biol Chem* 274: 12383–12390, 1999.
48. **Wang CY, Yang F, He X, Chow A, Du J, Russell JT, and Lu B.** Ca(2+) binding protein frequenin mediates GDNF-induced potentiation of Ca(2+) channels and transmitter release. *Neuron* 32: 99–112, 2001.
49. **Wei SK, Colecraft HM, DeMaria CD, Peterson BZ, Shang R, Kohout TA, Rogers TB, and Yue DT.** Ca^{2+} channel modulation by recombinant auxiliary beta subunits expressed in young adult heart cells. *Circ Res* 86: 175–184, 2000.
50. **Westenbroek RE, Hell JW, Warner C, Dubel SJ, Snutch TP, and Catterall WA.** Biochemical properties and subcellular distribution of an N-type calcium channel alpha 1 subunit. *Neuron* 9: 1099–1115, 1992.
51. **Yamaguchi H, Hara M, Strobeck M, Fukasawa K, Schwartz A, and Varadi G.** Multiple modulation pathways of calcium channel activity by a beta subunit. Direct evidence of beta subunit participation in membrane trafficking of the $alpha_{1c}$ subunit. *J Biol Chem* 273: 19348–19356, 1998.